21, rue d'Artois, F-75008 PARIS
http : //www.cigre.org
CIGRE US National Committee
2023 Grid of the Future Symposium

A Multi-Source Event Management Framework for Outage Detection and IBR Dynamic Performance Evaluation

J. KOUTSOURAIS, Y. LU and P. NIEVES
American Electric Power Service Corporation
USA

SUMMARY

Inverter-Based Resources (IBRs) are becoming more prevalent as the penetration of renewable generation continues to increase. With limited reactive capability and reduced inertia, renewable units introduce new challenges to today's power grid. With power electronics participating, system behaviors under faults slip into an unknown region, where adequate data are yet to be collected and proper standards are yet to be enacted. American Electric Power (AEP), as a transmission operator who doesn't dispatch generation from independent power providers, witnesses increasing uncertainty in system dynamic behavior as IBR integration trends upward. Therefore, it becomes increasingly imperative to monitor IBR response in states of system stress. Hence, with the purpose to enhance situational awareness and facilitate planning and regulatory actions, this paper proposes a framework for identification of moments of system stress and subsequent analysis, evaluation, and profiling of IBR dynamic performance.

With core structure consisting of a data-driven classification model, this framework cross references multiple data sources to identify and classify forced outage events, where system integrity is disrupted and operating limits of nearby IBRs can be tested. Fed from events generated and filtered by heuristically trained alarms watching rate of change on key system features, the classification model evolves to a 27-node decision tree with binomial targets addressing outage detection and categorization simultaneously. With the decision tree calibrated to desired precision via the Gini Impurity measure, system outages are captured and dynamic performances of nearby IBRs are swept for analysis.

Responses of IBRs are sorted by tracking the changes in generation immediately following an outage. Taking advantage of a python-based Graphic User Interface (GUI), dynamic responses of renewable units can be visualized and evaluated against existing IEEE standards and corporate integration agreements. Reliability profiles will be stablished where units responding positively in alleviating system stress shall be categorized as a source of support while their peers who failed to live up to integration agreements will be marked for future actions.

Configured and integrated in AEP since May 2023, the proposed multi-source framework reports 100 percent accuracy in outage identification and 94.5% accuracy in outage classification. With the purpose to achieve versatility, it continues to evolve with new data streamed in daily. Archives of IBR responses to outages are hence collected accordingly. As a consequence, unit profiles aggregate and will eventually propagate to all IBR units interconnected into AEP's transmission systems. Practicing a data

jmkoutsourais@aep.com

driven ideology, those profiles generalize dynamic characteristics of renewable resources. They will provide operators and engineers with intuitive understanding of unit potentials and possible impacts on the system. Eventually, those IBR profiles will serve both operation and planning departments and facilitate the enactment of new standards and agreements to enhance grid resilience against increasing renewable impacts in future power systems.

KEYWORDS

Gini Impurity Based Decision Tree, Inverter Based Resource (IBR), Outage Detection, Renewable Energy Source (RES), Renewable Unit Response

1. Introduction

With a rapid increase of renewable penetration in US power grids, more and more IBRs participate in grid operation. Currently, in Electricity Reliability Council of Texas (ERCOT)'s territory, renewables comprise approximately 30-45% of the total capacity on a given day [1]. Due to limitation in reactive capability and inertial response, renewable units bring uncertainty to power grids, particularly when systems are under stress [2]. Though equipped with capacitor banks and voltage regulators, IBR's response to system faults and equipment outages remains unpredictable, hindering situational awareness and sabotaging grid resilience. Therefore, it is essential to establish a mechanism where IBR's performance during system stress can be monitored, reported, and archived for future analysis.

Utilization of measurements to create a generator health profile has been explored for traditional generators [3,4], where sensors were deployed on the units to connect data reflecting electrical and physical characteristics. While the health profile provided a great reference for maintenance and replacement schedules, real-time performances of those units are yet to be explored from operation's point of view to ensure proper control schemes against potential instabilities. Supervisory Control and Data Acquisition (SCADA) data were utilized to remotely monitor the condition of wind turbines [5]. However, performance under system disturbances were not captured due to low sampling rate of SCADA measurement, leaving dynamic monitoring and reporting of IBRs incomplete.

Previous researchers have brought insights on tools and methods for fault diagnosis [6,7], where multiple data sources were queried and machine learning based algorithms were used. Nevertheless, due to limited renewable integration back then, IBRs' influences on system dynamic behaviors were negligible. Therefore, events suitable for testing IBR dynamic capability were not identified and RES unit behaviors under stress were not investigated nor evaluated. With increasing renewable penetration pushing transmission operation to newer limits today, fault detection and diagnosis shall be carried out with knowledges of impacts brought by IBRs.

AEP operates the nation's largest transmission system that absorbs over 1.9 GW of inverter-based generation [8]. Large amounts of power input from IBRs leads to increasing unpredictability concerning system behaviors in AEP's footprints, such as oscillations, delayed fault recoveries and even unplanned outages caused by lack of inertial response or reactive support. Monitoring, evaluating and documenting IBR performance, particularly under system stress, has hence been deemed highly necessary from both operation and planning perspectives. Fortunately, with over 500 PMUs deployed in its three footprints including ERCOT, Southwest Power Pool (SPP), and PJM, AEP benefits from a wide area PMU-based monitoring system that oversees Point of Interconnections (POI) of many IBRs, as shown in Figure 1.

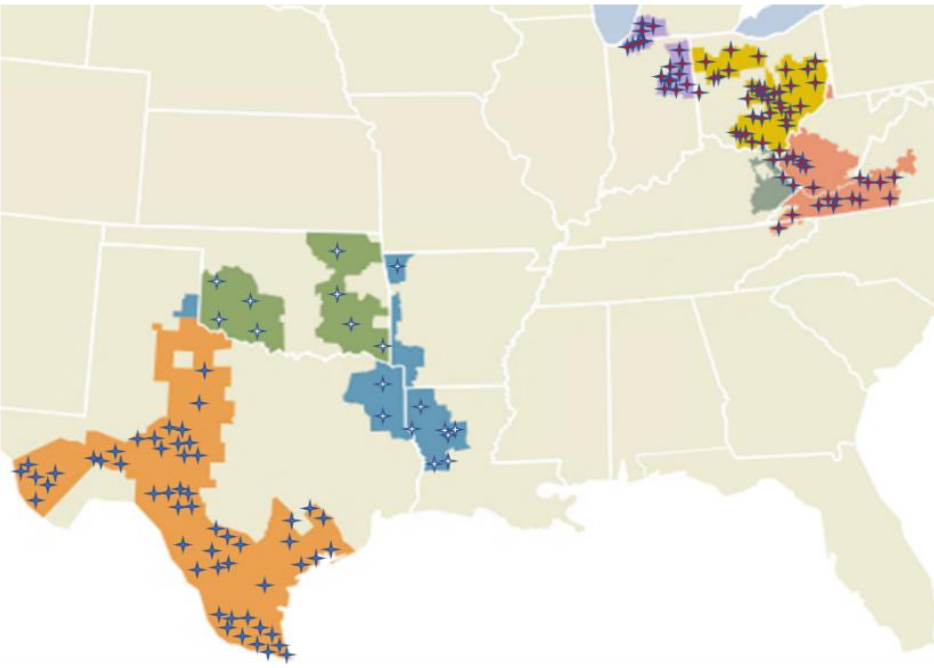

Figure 1 - PMU Monitored Substations of AEP

Taking advantage of the high-resolution observability enabled by PMUs, researchers at AEP have already developed measurement-based method to detect system oscillations [9]. To expand the scope of event detection and further extend the effort to enhance situational awareness and enrich operation knowledge, a multi-source event management framework is proposed. This framework automates detection and classification of critical events that disrupt system integrity and challenge IBR stability. IBR responses to those events are then recorded for evaluation. Reliability profiles for renewable units can hence be built to counter uncertainties introduced by renewables and enhance grid resilience.

2. Architecture

The multi-source framework is designed to capture and categorize system disturbances as well as report and profile IBR responses. Currently, we focus on disturbances that force permanent equipment outages as the loss of devices presents a concerning situation where operating limits of nearby IBRs are challenged. The framework feeds in information from three sources: a vendor supplied PMU application, an outage data repository, and a relay sequence data repository. The architecture of the proposed framework is displayed in Figure 2.

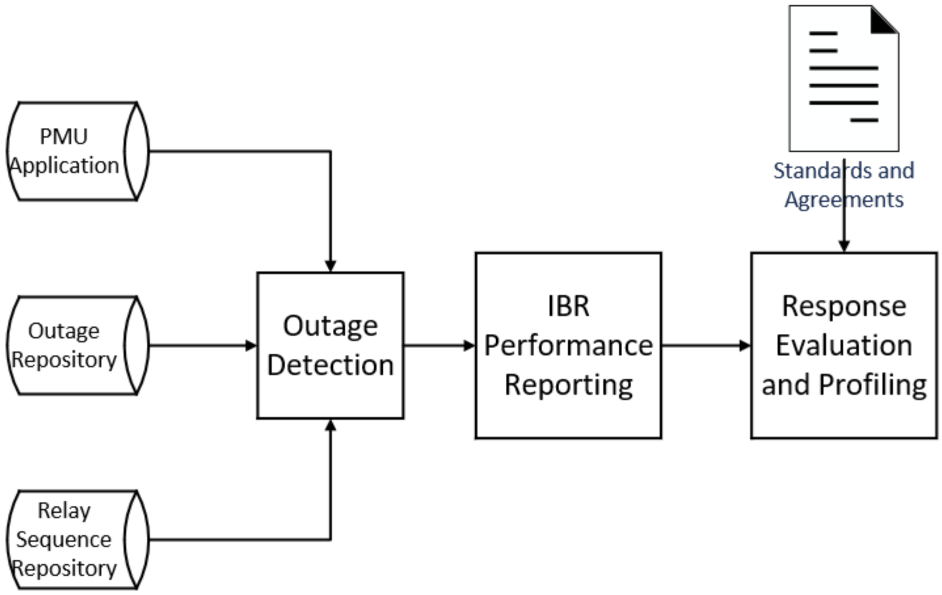

Figure 2 – Architecture of the Multi-Source Event Management Framework

As shown in Figure 2, cross referenced with three inputs, outage detection is carried out to identify system disturbances ideal for analyzing nearby IBR responses. The proposed framework is then completed with IBR response reporting and RES performance evaluation. Behaviors of units will be benchmarked with the IEEE standard concerning Interconnection of IBRs [10] and an internal renewable rating document [11], where interconnection requirements on real and reactive capability are detailed.

3. Methodology

To establish the proposed multi-source framework, real-time observations provided by PMUs as well as historical event data logged by outage and relay sequence repositories are both used to formulate the input and target of a decision tree-based event identification and classification model. The model is then refined and yields event notifications and characterizations that are adequately accurate for RES response evaluation and profiling.

A. Formulation

In order to generate an accurate model for outage detection and classification, system conditions must be generalized and parameterized as inputs to model learning [12]. To sufficiently include dynamic features of a disturbance in model refining, absolute differences of pre and post fault features as well as Rate of Changes (ROC) during faults are used to formulate the input array.

AEP's existing wide-area monitoring system (WAMS) detects approximate event time $t_i^{Detected}$ using empirical ROC alarms, which are triggered instantly when ROC values touch the lowest threshold. To find the exact event time $t_i^{Corrected}$, locations and timestamps of observations reflecting the maximum ROC values are sought via (1)-(6), where a rolling window analysis is carried out with 500 samples timestamped before and after $t_i^{Detected}$ are screened:

$$\overline{V_i^H} = \{V_{i-H}, V_{i-H+1}, \dots, V_{i+H}\} \tag{1}$$

$$V_{ROC_i}^{1s} = |V_i - V_{i+30}| \tag{2}$$

$$V_{ROC}^{1s} = \max_{i-H \le n \le i+H} \{V_{ROC_n}^{1s}\} \tag{3}$$

As H=500, $\overline{V_i^H}$ hosts one thousand and one voltage observations surrounding detected event time with V_i timestamped at $t_i^{Detected}$. Using a window length of one second that hosts 30 samples, absolute difference reported between the first samples of two consecutive windows are then calculated to obtain instantaneous voltage ROC $V_{ROC_i}^{1s}$ at $t_i^{Detected}$. With observation window moving through $\overline{V_i^H}$, a series of $V_{ROC_n}^{1s}$ will be computed. The final ROC concerning voltage is represented as V_{ROC}^{1s}. It equals the numerical maximum of $V_{ROC_n}^{1s}$.

Similarly, f_{ROC}^{1s} and $P_{\%ROC}^{1s}$ represent rates of change concerning frequency and active power respectively. They are derived via the same rolling window method with $P_{\%ROC}^{1s}$ processed by an additional division step to obtain the percent change:

$$f_{ROC}^{1s} = \max_{i-H \le n \le i+H} \{f_{ROC_n}^{1s}\} \tag{4}$$

$$P_{\%ROC_i}^{1s} = \left|\frac{P_i - P_{i+30}}{P_i}\right| \tag{5}$$

$$P_{\%ROC}^{1s} = \max_{i-H \le n \le i+H} \{P_{\%ROC_n}^{1s}\} \tag{6}$$

Timestamps of V_{ROC}^{1s}, f_{ROC}^{1s}, and $P_{\%ROC}^{1s}$ mark the corrected event time $t_i^{Corrected}$. Since topology information constitutes part of PMU names, signals reporting alarming ROC values pinpoint event locations as well. With $t = t_i^{Corrected}$, input variables concerning pre and post event system conditions are formulated as:

$$\Delta V_{Fault} = V_{t_0} - V_{t_{-1}} \tag{7}$$

$$\Delta P_{\%Fault} = \frac{P_{t_0} - P_{t_{-1}}}{P_{t_{-1}}} \tag{8}$$

$$\Delta P_{\%Post\ Fault} = \frac{P_{t_1} - P_{t_{-1}}}{P_{t_{-1}}} \tag{9}$$

$$\Delta P_{\%Recovery} = \frac{P_{t_2} - P_{t_{-1}}}{P_{t_{-1}}} \tag{10}$$

Where $V_{t_{-1}}$ and $P_{t_{-1}}$ are pre-fault voltage and active power, V_{t_0} and P_{t_0}represent system features immediately after faults, $P_{t_1}$and P_{t_2} denote short-term and long-term post-fault active power respectively. Here, ΔV_{Fault} and $\Delta P_{\%Fault}$ indicate the severity of the fault, while $\Delta P_{\%Post\ Fault}$ and $\Delta P_{\%Recovery}$ differentiate permanent outages from temporary ones. Pre and post fault change on voltage and active power, together with their ROC thresholds, form the input array. Referred to as X_{DT}, The input array summarizes grid conditions before, during, and post disturbances.

$$X_{DT} = [\Delta V_{Fault}, \Delta P_{Fault}, \Delta P_{Post\ Fault}, \Delta P_{Recovery}, V_{1s\ ROC}, f_{1s\ ROC}, P_{1s\ \%Change}] \tag{11}$$

B. Training

A Gini Impurity Based Classification Tree [13] is built and trained to create the model for event identification and characterization. The training starts with initialization of ROC thresholds to bypass benign system fluctuations. The initialized thresholds are listed in Table 1:

Table 1 - Initial Thresholds

$V_{ROC}^{Threshold}$	$.05\,\frac{PU}{s}$
$P_{\%ROC}^{Threshold}$	$\frac{10\%\ Change}{s}$
$f_{ROC}^{Threshold}$	$.5\,\frac{Hz}{s}$

With initialized ROC thresholds, system disturbances flagged by empirical ROC alarms are filtered, however, not all filtered events are equipment outages. Using E_I to denote all events flagged by empirical alarms, E_C and E_{NA} are subsets of E_I as they represent outage and non-outage events respectively. With $E_{Undetected}$ referring to missed outage events, different sets of events exhibit relationships depicted as (12) and (13).

$$E_I \equiv E_C \cup E_{NA} \tag{12}$$
$$E_{Outage} \equiv E_C \cup E_{Undetected} \tag{13}$$

With X_{DT} as an input array, the Gini Impurity based classification tree aims to capture all 'severe' events that force equipment outages as well as classifying them based on event causes and outage types. Supplying outage characteristics and incidence causes as part of the objective functions, AEP's outage repository and relay sequence logs are constantly scanned during the learning procedure to cross reference events filtered via ROC alarms and provide feedback to model training. Thresholds defining ROC alarms will be heuristically adjusted until E_{Outage} equals to E_C. As a result, $E_{Undetected}$ becomes an empty set.

Aiming for detection as well as classification, a weighted Gini index is computed for each variable in the input array to decide the optimal split at each node. Consequently, the decision tree evolves to a binominal target model. Its training is completed by adopting the python's scikit-learn package [14], where the procedure is elaborated in Figure 3. Sampling data is split into training and testing subsets. The classification tree is calibrated with the training set and validated with the testing one.

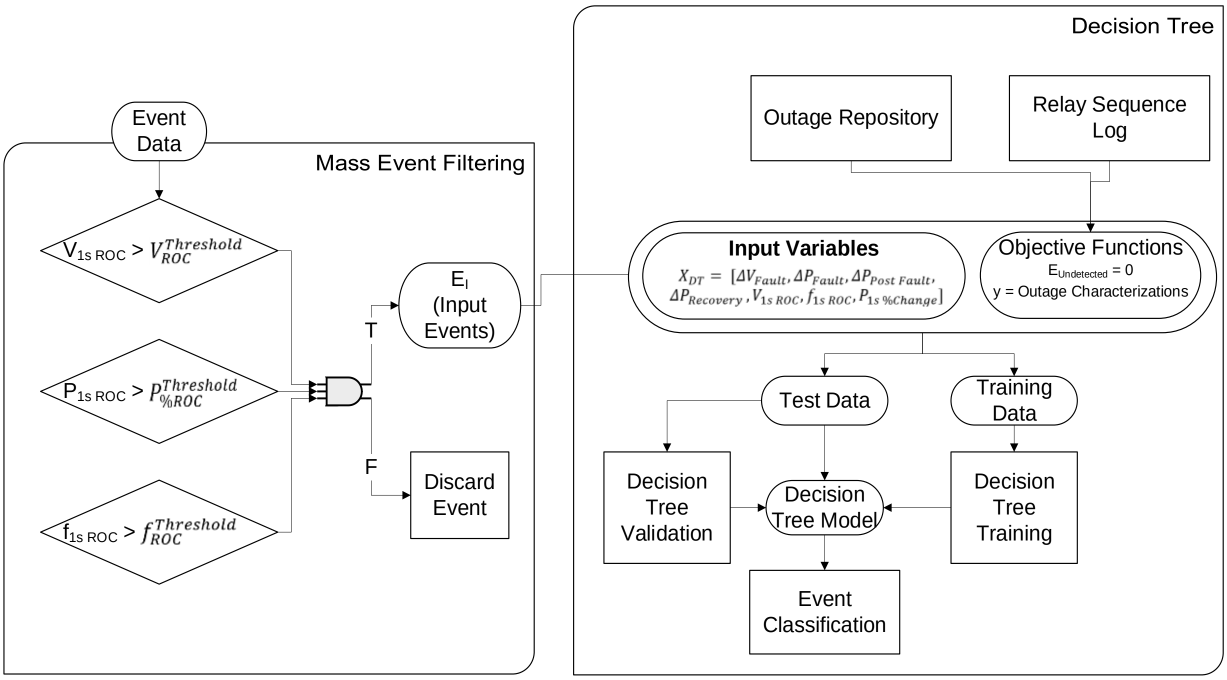

Figure 3 - Filtering and Decision Tree Structure

C. Reporting

Following outage detection and classification, renewable units within proximity of detected outages are swept and analyzed using a similar rolling window method as described in (1)-(2). Event induced changes in RES outputs are measured using $\bar{P}_{ROC}^{1s}$ and $\bar{Q}_{ROC}^{1s}$, which are average rate of change concerning real and reactive power in response to outages. With $J = 150$, three hundred observations surrounding $t_i^{Corrected}$ are scrutinized as formulated in (16) and (19). Responses are then sorted accordingly based on unit average ROC concerning real and reactive outputs. The sweeping and reporting procedure of RES responses is visualized in Figure 4.

$$P_{ROC_{i-J}}^{1s} = \left|P_{i-J} - P_{i-J+30}\right| \tag{14}$$

$$P_{ROC}^{1s} = \left\{P_{ROC_{i-J}}^{1s}, P_{ROC_{i-J+1}}^{1s}, \dots, P_{ROC_{i+J}}^{1s}\right\} \tag{15}$$

$$\bar{P}_{ROC}^{1s} = \frac{\sum_{i-J}^{i+J} P_{ROC}^{1s}}{2J} \tag{16}$$

$$Q_{ROC_{i-J}}^{1s} = \left|Q_{i-J} - Q_{i-J+30}\right| \tag{17}$$

$$Q_{ROC}^{1s} = \left\{Q_{ROC_{i-J}}^{1s}, Q_{ROC_{i-J+1}}^{1s}, \dots, Q_{ROC_{i+J}}^{1s}\right\} \tag{18}$$

$$\bar{Q}_{ROC}^{1s} = \frac{\sum_{i-J}^{i+J} Q_{ROC}^{1s}}{2J} \tag{19}$$

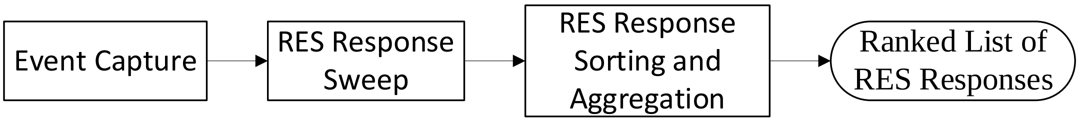

Figure 4 - Fetching RES Responses

Following unit sweeping, profiles for each renewable are manually built to include:

- Archival of event data for future references and studies
- Plots of RES responses for evaluation of unit dynamic performance
- Operating power factor vs. rated power factor at different ratings to benchmark RES active and reactive capability with standards and integration requirements.

4. Implementation

The proposed framework incorporates a vendor-supplied PMU WAMS software, where real-time ROC events triggered by empirical alarms are streamed to the Gini Impurity based classification tree. With model training completed, the classification tree memorizes its targets and generates desired outcomes with inputs concerning static and dynamic grid conditions.

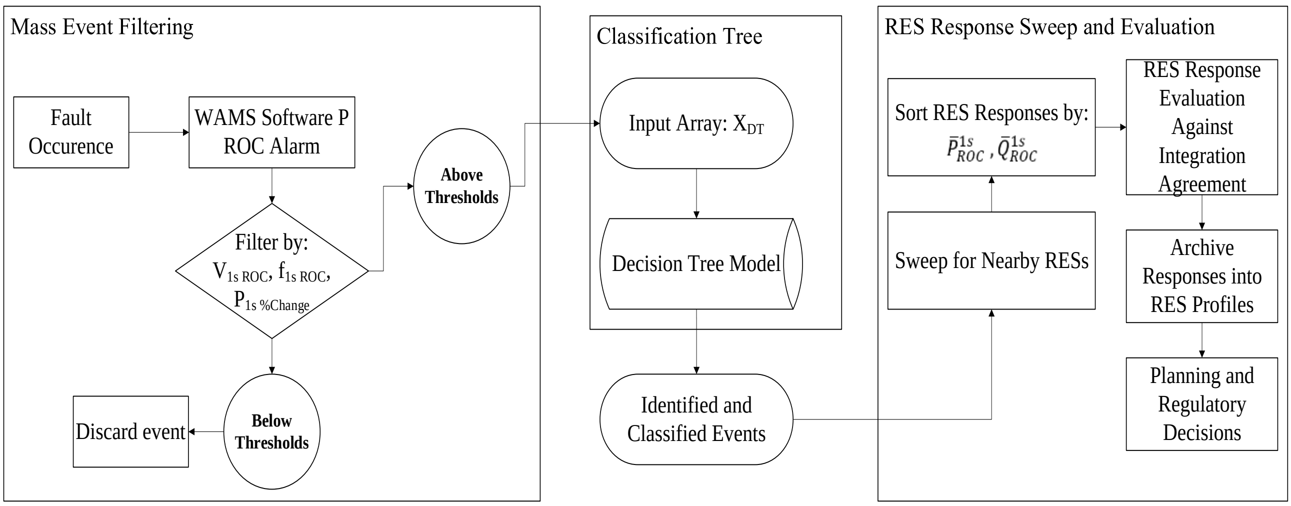

Figure 5 – Implementation Procedure

The implementation of the proposed framework is divided into 3 subprocesses as shown in Figure 5:

1. ***Mass Event Filtering*** –System fluctuations marked by empirical ROC alarms over a 30-day period are gathered, grouped, and filtered to reduce the dimension of the input array and suppress perturbations to the framework.
2. ***Decision Tree Based Outage Detection and Classification*** –The input array consisting of ROCs and pre/post fault changes is fed into a well-tuned decision tree, which identifies disturbances that force permanent outages. Those disturbances are classified using a list of event causes including lightning, tornado, line overheat, and so on.
3. ***RES Response Sweep and Evaluation*** – Dynamic responses from RESs near identified outages are swept, analyzed, and sorted. With a python-based GUI producing time domain plots as shown in figure 6, each RES's capability in providing real and reactive power support to mitigate system stress is scrutinized. Profiles characterizing their dynamic performances will hence be built to justify planning and regulatory actions.

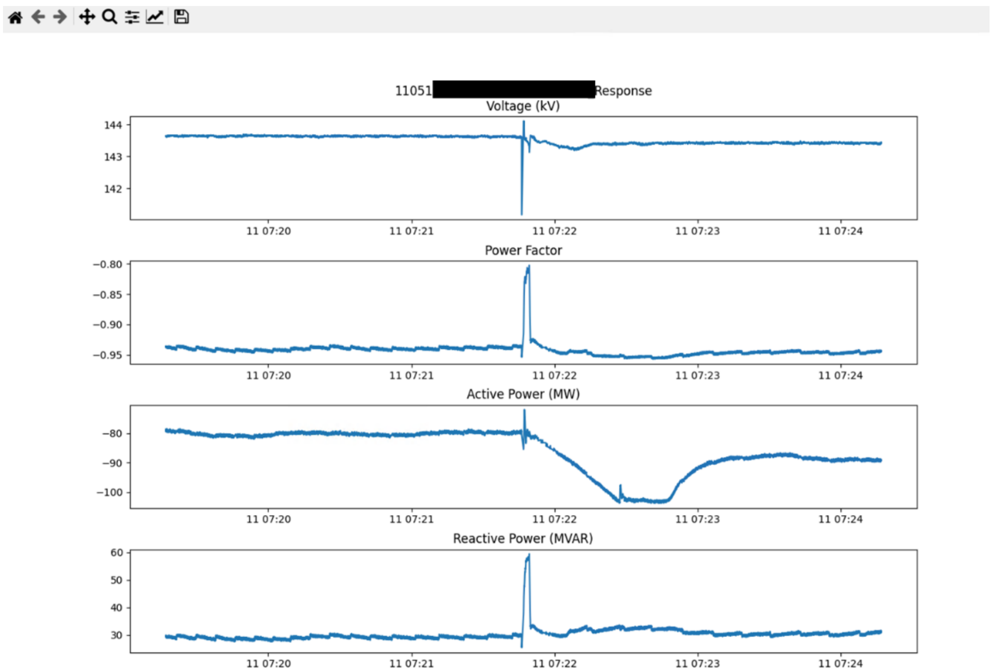

Figure 6 - Renewable Response Decision GUI

Since the decision tree is trained offline with multiple databases calibrating its output, it delivers decent accuracy in terms of outage detection and classification. By design, cross references with outage repository and relay sequence logs shall no longer be necessary once training is finalized with adequate thoroughness and diversification. The calibrated decision tree shall then work on its own to realize and maintain desired precision despite evolving system conditions. This ideology is purely data-driven, it reduces communication effort and simplifies process flow, equipping the proposed framework with real-time adaptability.

5. Performance Evaluation

The performance of the proposed multi-source framework was evaluated via validating outputs from the decision tree as well as analyzing the captured RES responses. Though preliminary, the latter demonstrated functionality of the proposed framework.

A. Decision Tree Model Validation

Over a period of 30 days, 486 events prefiltered from 33,585 empirical ROC-based notifications were fed into the binomial target decision tree. Out of which 340 events were used for learning and the rest used for testing. The calibrated classification model eventually grew to be a 27-node decision tree

It successfully flagged 32 PMUs reflecting all 6 outages blended in with non-outage disturbances in the event cluster created for testing, yielding 100 percent accuracy concerning outage identification.

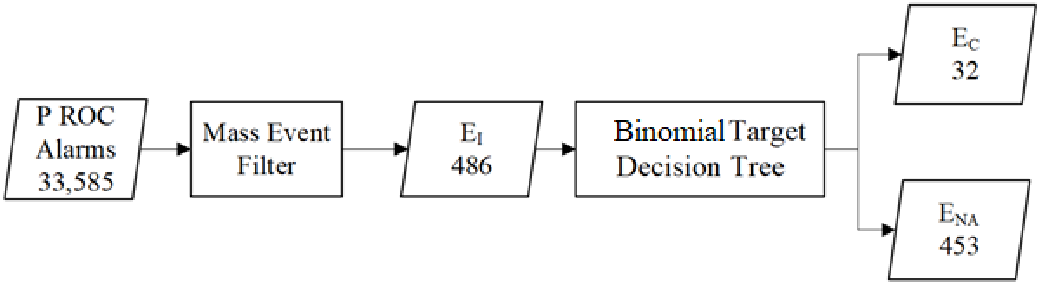

Figure 7 – Decision Tree Model Validation

As for outage classification, four different outage causes (Tornado, Lightning, Line Overheat, Other) plus five different outage types (manual, forced, temporary, permanent, non-outage) created 20 possible combinations for each of the 146 events clustered for testing. The finalized decision tree delivered the correct combination for 138 out of 146 events, indicating 94.5% accuracy. A visualization of the 27-node decision tree is displayed as Figure 10 in the appendix.

B. IBR Responses

The 6 outage instances had in total 8 renewable responses observed by PMUs at or next to their POIs. In this round of outage detection and RES evaluation, no renewable units were seen operating at or above their max P or Q capacity nor operating at below 10% of their real power capability. With no extreme case presenting, the responses were split into "P Support" and "Q Support" categories in Table 2. The magnitude of each response was recorded along with the event location in Table 3.

Table 2 - Event Renewable Responses

Event	**Number of PMUs Flagged**	**Highest V_{ROC}^{1s} Captured at PMU#**	**Responses**	**Event Classification**
1	2	10038	2 P Support, 1 Q Support	Tornado
2	2	10075	1 P Support	Lightning
3	1	11050	None	Lightning
4	2	10060	1 P Support	Lightning
5	2	11130	1 Q Support	Other
6	23	10042	2 P Support	Line Overheat

Table 3 - RES Response Summary

Response (PMU ID)	**Category – Description**	**Machine Type**	**Min. PF**
Event 1 – 1 (10059)	P Support – 21.4MW increase	Wind – Type Unknown	.98
Event 1 – 2 (10086) operating at ~95%	P Support – 13.6MW increase	Wind – Type 3	.96
Event 1 – 3 (11051) operating at ~60%	Q Support – 45.1MVAR increase	Wind – Type 3	.45
Event 2 – 1 (11054) operating at ~50%	P Support – 9.7MW increase	Wind – Type Unknown	.99
Event 4 – 1 (11051) operating at ~50%	P Support – 22.1MW increase	Wind – Type 3	.91
Event 5 – 1 (11160) operating at ~80%	Q Support – 6.4 MVAR increase	Wind – Type 3	.93
Event 6 – 1 (10059)	P Support – 250 MW increase	Wind – Type Unknown	1
Event 6 – 2 (11051) operating at 40%	P Support – 24.5 MW increase	Wind – Type 3	.8

Though only required to provide limited reactive support corresponding to ±0.95 power factor at POI, the wind farm observed by PMU #11051 demonstrates capability to operate and interconnect at a much lower power factor when necessary, providing more dynamic support to transmission grids compared with other wind units powered by doubly fed asynchronous turbines. This RES is hence profiled as a potential reactive resource for AEP's ERCOT system. Its responses to Event 1 and 6 are plotted in Figures 8 and 9 respectively.

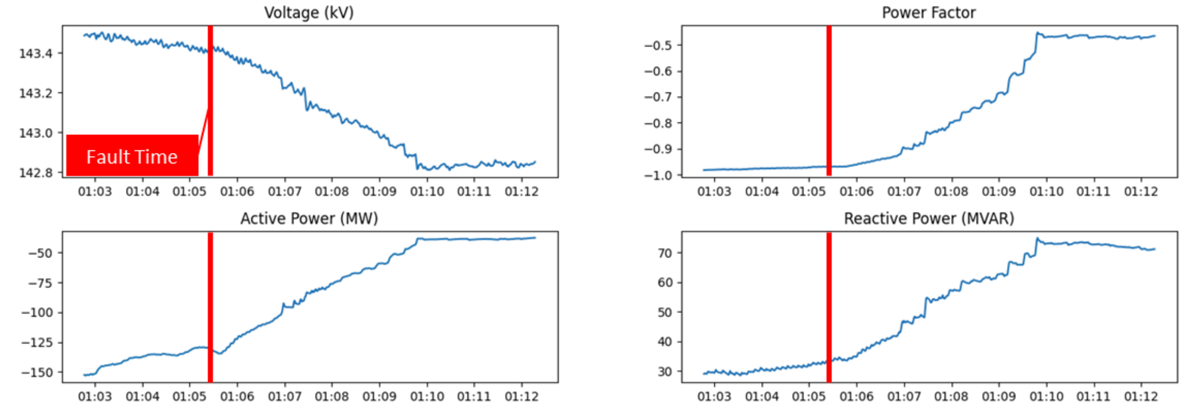

Figure 8 - Event 1 Response - PMU 11051

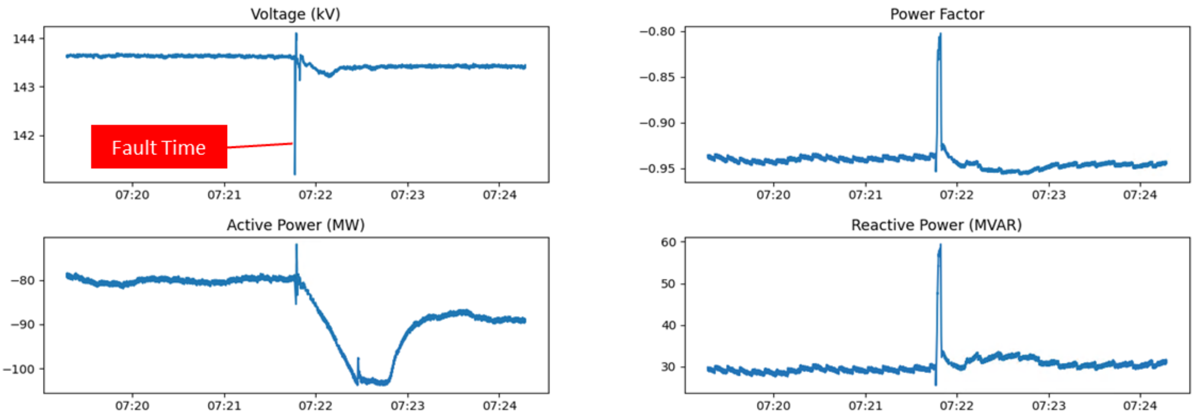

Figure 9 - Event 6 Response - PMU 11051

Event 1 was caused by a tornado that took out a 69kV line for approximately 62 hours. While the wind farm observed by PMU 11051 is located further from the event than other renewable resources and traditional generators, it increased reactive output by 45.1 MVAR within 5 minutes, stabilizing voltages in affected area and demonstrating promising Automatic Voltage Control (AVR) functions. Event 6 was caused by a line overheat that put a major 345kV line out of service for over 26 hours. With a critical path to generation out, the wind farm observed by PMU 11051 ramped up active power output to 105 MW in less than a minute following the line outage, adding 13% of its capacity to compensate for loss of generations and demonstrating resilience under stressed situations. Hereby, this wind farm is archived as a reliable IBR to facilitate operation and planning actions.

6. Conclusion

This paper established a multi-source framework for outage detection, classification and RES response evaluation. With a binomial target decision tree serving as its core feature. The framework demonstrates promising performance where 100 percent accuracy in outage detection and 94.5% accuracy in outage classification can be achieved. As a result, the proposed framework demonstrates ability to capture severe disturbances in real time with dynamic responses from nearby IBRs monitored, evaluated, and archived. Reliability profiles can hence be established for multiple IBRs where potential sources of support or troublemakers can be identified to enrich control room knowledge and provide reference for planning and regulatory actions. The contribution of the paper can be summarized as below:

1. Building and calibration of a binomial target classification model with real-time adaptability to realize fast and accurate outage detection and categorization.
2. Establishing a multi-source framework to automate IBR dynamic response monitoring, reporting, and reliability profiling.
3. Proposal of a data-driven ideology to generalize RES dynamic characteristics, supplementing control room knowledge, and facilitating long term actions to enforce grid resilience.

With event data queried and streamed to the multi-source framework on a daily basis, the decision-tree-based outage identification and classification model will continue its evolvement to achieve versatility. Meanwhile, the archival of IBR responses will continue to aggregate. Reliability analysis and profiling will eventually propagate to all RES units interconnected to AEP’s transmission system. Those profiles will benefit system operation and planning, as well as facilitate the enactment of new interconnection standards accommodating a future grid with increasing renewable penetration.

7. Appendix

A visual representation of the selected decision tree is depicted in Figure 10. Characteristic splitting features, Gini Impurity values, number of samples, feature variable values, and deciding classes are displayed at each node.

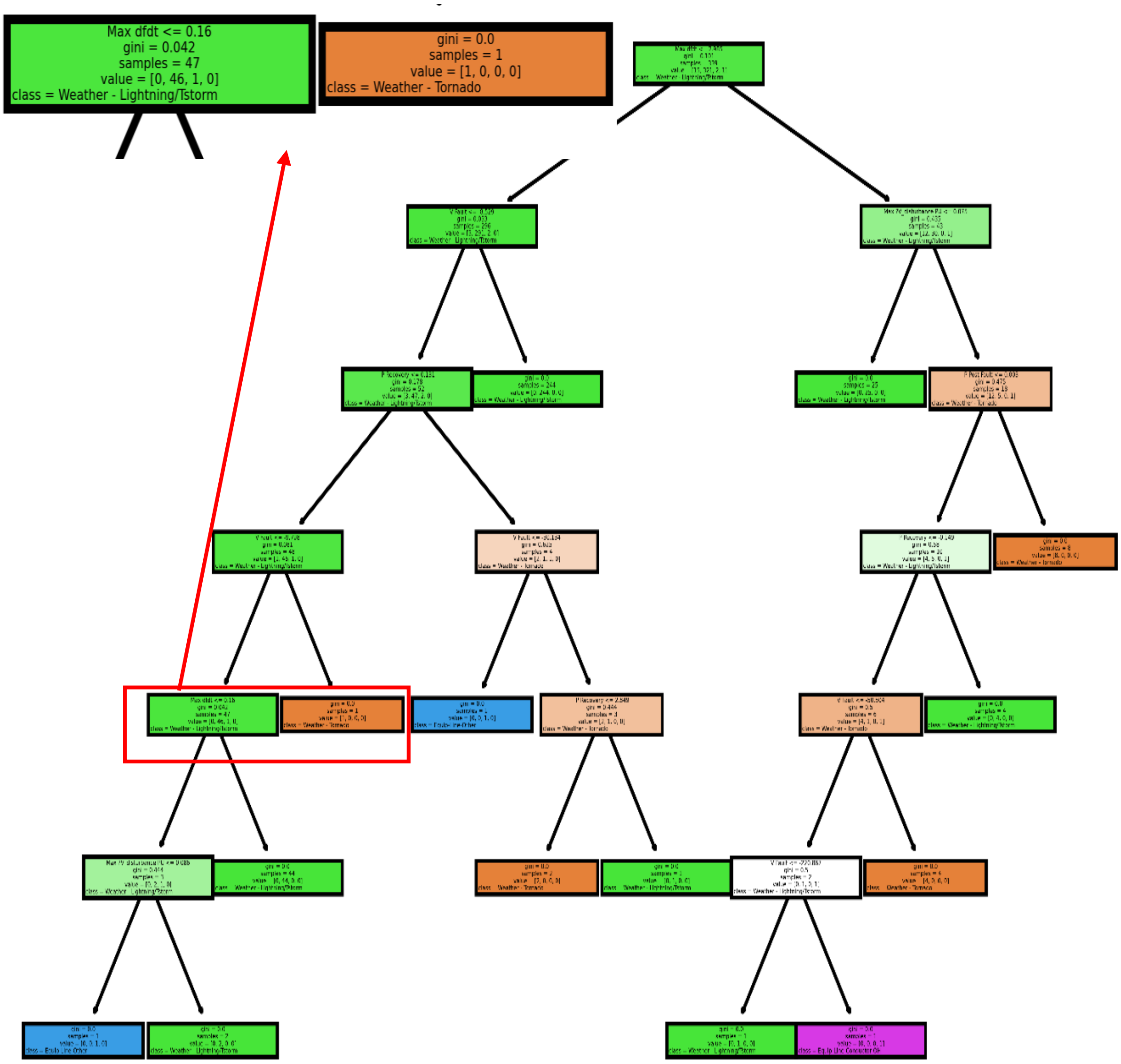

Figure 10 – Decision Tree Visualization

BIBLIOGRAPHY

[1] “Renewable Integration Report,” ercot.com https://www.ercot.com/mp/data-products/data-product-details?id=NP4-760-ER (accessed Jul. 18, 2023).

[2] E. F. Areed and I. Alcaide-Godinez, "Large-Scale Renewable Energy Penetration Impact on System Stability," 2021 IEEE PES Innovative Smart Grid Technologies - Asia (ISGT Asia), Brisbane, Australia, 2021, pp. 1-5, doi: 10.1109/ISGTAsia49270.2021.9715605.

[3] B. Ali, A. A. Khan, M. H. Baig, S. Ahmed, D. Hussain and M. Waqas, "Remote Monitoring and Index Based Maintenance Scheduling of Domestic Gasoline Generators for loss Reduction Using Android Application," 2021 International Conference on Emerging Power Technologies (ICEPT), Topi, Pakistan, 2021, pp. 1-5, doi: 10.1109/ICEPT51706.2021.9435510."

[4] P. W. Tse, E. Y. Li, J. C. Chan and J. T. Leung, "Automatic generator health assessment system that embedded with advanced fault diagnosis and expert system," 2010 Prognostics and System Health Management Conference, Macao, China, 2010, pp. 1-7, doi: 10.1109/PHM.2010.5413425.

[5] X. Jin, Z. Xu and W. Qiao, "Condition Monitoring of Wind Turbine Generators Using SCADA Data Analysis," in IEEE Transactions on Sustainable Energy, vol. 12, no. 1, pp. 202-210, Jan. 2021, doi: 10.1109/TSTE.2020.2989220.

[6] Y. N. Wang, J. F. Ye, G. J. Xu, Q. M. Chen, H. Y. Li and X. R. Liu, "Novel hierarchical fault diagnosis approach for smart power grid with information fusion of multi-data resources based on fuzzy petri net," 2014 IEEE International Conference on Fuzzy Systems (FUZZ-IEEE), Beijing, China, 2014, pp. 1183-1189, doi: 10.1109/FUZZ-IEEE.2014.6891791.

[7] A. Jain, T. C. Archana and M. B. K. Sahoo, "A Methodology for Fault Detection and Classification Using PMU Measurements," 2018 20th National Power Systems Conference (NPSC), Tiruchirappalli, India, 2018, pp. 1-6, doi: 10.1109/NPSC.2018.8771757.

[8] “AEP Renewables,” aep.com https://www.aep.com/about/businesses/aeprenewables (accessed Jul. 18, 2023).

[9] Y. Lu, Y. Kong, and F. Tu “A KDE-based Methodology for PMU Data Management and Real-time Event Detection,” CIGRE Paris Session, Paris, France,

[10] "IEEE Standard for Interconnection and Interoperability of Inverter-Based Resources (IBRs) Interconnecting with Associated Transmission Electric Power Systems," in *IEEE Std 2800-2022*, vol., no., pp.1-180, 22 April 2022, doi: 10.1109/IEEESTD.2022.9762253.

[11] Voltage and Reactive Guidelines, EDOPS.01.115.00_GUI, American Electric Power Company, Inc., 4/21/2023.

[12] Suthaharan, Shan, and Shan Suthaharan. "Decision tree learning." Machine Learning Models and Algorithms for Big Data Classification: Thinking with Examples for Effective Learning (2016): 237-269.

[13] D’Ambrosio, Antonio, and Valerio A. Tutore. "Conditional classification trees by weighting the Gini impurity measure." In New Perspectives in Statistical Modeling and Data Analysis: Proceedings of the 7th Conference of the Classification and Data Analysis Group of the Italian Statistical Society, Catania, September 9-11, 2009, pp. 273-280. Springer Berlin Heidelberg, 2011.

[14] “Decision Trees”, scikit-learn.org https://scikit-learn.org/stable/modules/tree.html#id2 (accessed Jul. 19,2023)